2011 IEEE International Conference on Robotics and Automation
Shanghai International Conference Center
May 9-13, 2011, Shanghai, China

Design of the Pendulum Juggler

Philipp Reist and Raffaello D'Andrea

Abstract— **We present the analysis and design process of the Pendulum Juggler, a robot that juggles a ball with an actuated paddle mounted to a swinging pendulum. The unconstrained ball travels up to 1 m horizontally, reaching an apex height of 1.1 m between impacts. Using a perturbation analysis, we show that the ball trajectory is locally stable without feedback. The pendulum consists of a four-bar linkage, optimized to keep the paddle perpendicular to the impact velocity of the ball. We verify the stability in experiments with a prototype of the Pendulum Juggler, demonstrating sustained juggling at amplitudes of up to 25°.**

I. INTRODUCTION

In 2009, we developed the Blind Juggler, a robot that is able to vertically bounce an unconstrained ball on a paddle that is actuated by a linear motor [1]. The Blind Juggler can bounce a ball at heights of up to 2.1 m without any sensors to measure the ball state. Two design parameters provide stability to the system: 1) a concave parabolic paddle keeps the ball from bouncing off the robot, and 2) a decelerating paddle at impact stabilizes the ball's apex height. We first found the parameters with a local stability analysis, and later optimized them using an H_2-norm metric. This resulted in minimized standard deviations of the apex height and impact location distributions of the ball.

Using these results, we are now designing a new device, the Pendulum Juggler, which further explores the boundary of what is possible with open-loop juggling. We mount the paddle and linear motor of the Blind Juggler to a pendulum-like linkage that swings at amplitudes of up to 30°. The ball is struck at the peak angles of the pendulum; therefore, the ball travels up to 1 m horizontally and reaches an apex height of 1.1 m in between impacts. This is illustrated in Fig. 1.

The system provides a rich control problem. The pendulum needs to be synchronized with the striking motion of the paddle. We currently use motors to exert a torque on the pendulum, combined with a simple proportional controller for synchronization. We may use the Pendulum Juggler to test more advanced controllers for synchronization, for example the controller presented by Schöllig et al. [2] to synchronize the motion of a flying vehicle to music. In addition to the motors, we could make use of the influence the paddle motion has on the pendulum dynamics, i.e. the same physics as children exploit on swings (which have been studied, e.g. recently by Piccoli et al. [3]). Similarly, we could use the part of the paddle trajectory that is not constrained by the striking motion to control the pendulum's motion. Ideally, this would make the motors redundant.

The authors are with the Institute for Dynamic Systems and Control, ETH Zurich, Switzerland. Supporting material, including videos, may be found at www.blindjuggler.org.

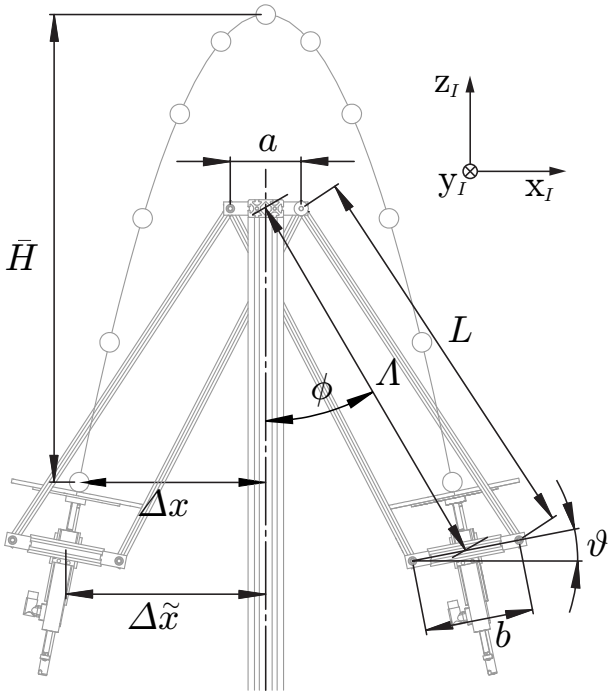

Fig. 1. The Pendulum Juggler. The illustration shows the nominal trajectory of the ball. Also depicted are: the equivalent pendulum angle ϕ and length Λ; the four-bar linkage parameters a, b, and L; the paddle angle ϑ.

Juggling robots have been used to validate new control algorithms, such as the work by Burridge et al. on sequential controller design [4] or the mirror law introduced by Bühler et al. [5]. Rizzi et al. generalized the mirror law to unconstrained balls and achieved simultaneous juggling of two balls with a direct drive robot arm, the Bühgler, and vision feedback [6]. In contrast to systems featuring constant ball tracking, open-loop juggling systems have been analyzed in dynamics research, e.g. by Holmes [7], and recent work in robotics by Schaal et al. [8]. Most notable is the work by Ronsse et al. [9], [10] with the Wiper robot, which is similar to the Pendulum Juggler. The Wiper consists of two actuated aluminum beams and juggles discs on a tilted air-hockey table. It juggles feed-forward or with feedback using measured impact times, and can even generate a juggling pattern similar to the shower pattern, where the balls are in a circular motion.

With respect to existing work in robotic juggling, the distinctive feature of the Pendulum Juggler is that it juggles unconstrained balls with a single paddle in a side-to-side pattern without feedback.

Lastly, open-loop juggling can be compared to passive

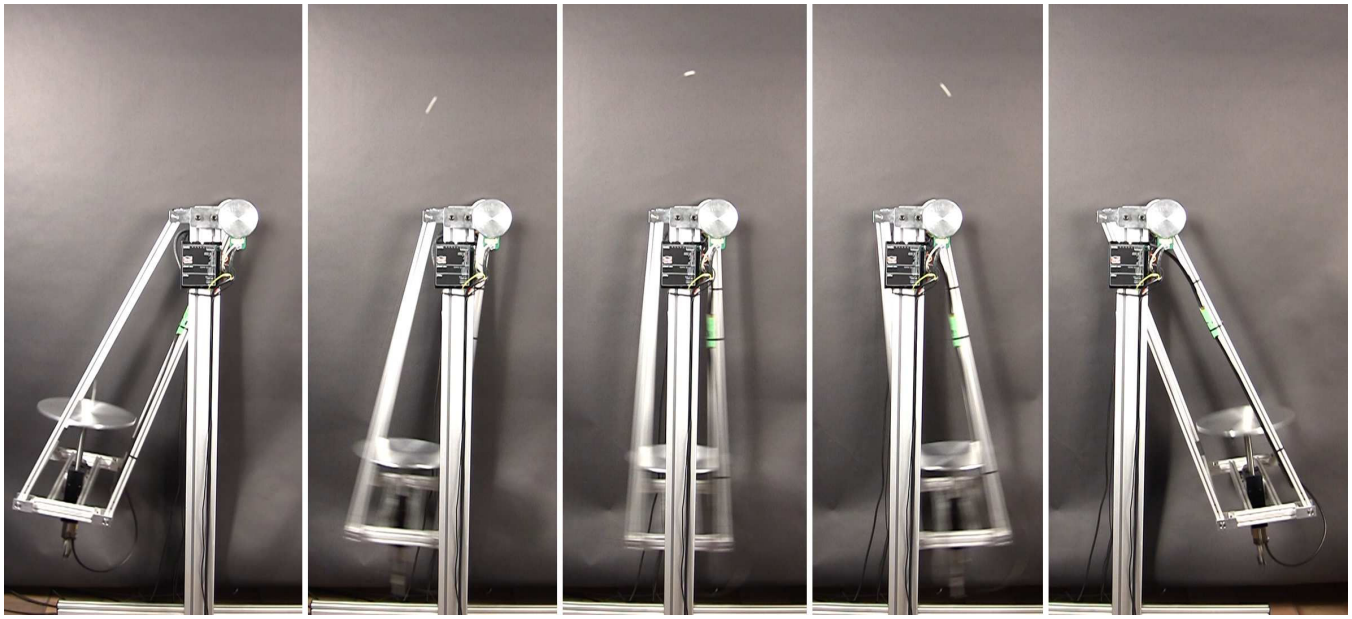

Fig. 2. The Pendulum Juggler juggling at an amplitude of 25°. The round structures at the top are brushless motors controlling the pendulum motion.

dynamic walking and running robots, which feature stabilizing mechanisms that allow them to walk or run down a slope without any actuators or sensors. One recent example is the work of Miyamoto et al, who studied the dynamics and stability of a glass fiber rod running down a slope [11].

The design process of the Pendulum Juggler starts with the calculation of the nominal ball trajectory in Section II. We then analyze the trajectory's local stability using a perturbation analysis in Section III. Next, we discuss the hardware design, paying particular attention to the four-bar linkage in Section IV. Finally, we present preliminary experimental results with the completed system in Section V.

II. NOMINAL TRAJECTORY

Before analyzing stability, we establish the nominal ball trajectory illustrated in Fig. 1. As we do not yet have the four-bar linkage geometry available, we use a simplified structure of the Pendulum Juggler defined by an equivalent pendulum angle ϕ and length Λ (see Fig. 1) in the following calculations. We find the nominal flight time of the ball from apex to impact to be

$$T = \sqrt{\frac{2\bar{H}}{\gamma}}, \tag{1}$$

where $\gamma = 9.81\,\mathrm{m\,s^{-2}}$ is the gravitational acceleration and $\bar{H}$ is the nominal apex height of the ball. The pendulum period is therefore $4T$. We assume aerodynamic effects on the ball (such as air drag) to be negligible. Therefore, the constant nominal horizontal velocity of the ball during flight is

$$\bar{v}_{Sx} = \frac{\Delta\tilde{x}}{T} = \frac{\Lambda \sin\Phi}{T}, \tag{2}$$

where Φ is the equivalent pendulum's amplitude and $\Delta\tilde{x}$ is half the horizontal distance the ball travels between impacts. The vertical ball velocity just before impact is

$$\bar{v}_{Sz} = -\sqrt{2\gamma\bar{H}} = -T\gamma. \tag{3}$$

The paddle needs to be perpendicular to the impact velocity of the ball. Therefore, the nominal paddle angle is

$$\bar{\vartheta} = \arctan\frac{\bar{v}_{Sx}}{\bar{v}_{Sz}}. \tag{4}$$

The magnitude of the impact velocity is

$$|\bar{v}_S| = \sqrt{\bar{v}_{Sx}^2 + \bar{v}_{Sz}^2}. \tag{5}$$

Therefore, the nominal paddle speed at impact is

$$\bar{v}_P = |\bar{v}_S|\frac{1-e_z}{1+e_z}, \tag{6}$$

which we obtain from Newton's impact law

$$|\bar{v}_S| = e_z|\bar{v}_S| + (1+e_z)\bar{v}_P, \tag{7}$$

where we assume that the ratio of the ball mass to the paddle mass is negligible (the ratio for the given robot is 3×10^{-4}).

III. PERTURBATION ANALYSIS

We show that the nominal trajectory is locally stable by deriving a linearization of the Poincaré map that describes how perturbations added to the nominal apex state of the ball map over an impact to the next apex. The linearization is derived using first order approximations to the system equations. Because the second segment of the ball trajectory is just a mirrored version of the first, it is sufficient to only analyze the ball trajectory from apex to apex over a single impact. The nominal trajectory is locally stable if the spectral radius of the derived map is smaller than one [12].

Because the map is derived in two dimensions, the ball state for the analysis is $S = [x, \dot{x}, \omega_y, z, \dot{z}]$, where ω_y is the

ball spin. The spins $\omega_x, \omega_y, \omega_z$ are defined by the right-hand rule in the coordinate system shown in Fig. 1. We showed in previous work that the planar, first order analysis generalizes to three dimensions for vertical juggling. The ball degrees of freedom in $y, \dot{y}$, and ω_x are not affected by the nominal paddle angle $\bar{\vartheta}$ and are therefore stable as derived in [1].

A. Introduce Perturbations

The perturbations s_0 are added to the nominal initial conditions of the ball

$$S_0 = \bar{S}_0 + s_0, \tag{8}$$

where the subscript 0 denotes the initial apex time. In the following, the ball state and perturbations are always expressed in the inertial coordinate system I. The nominal initial conditions are

$$\bar{S}_0 = \left[-\Delta\tilde{x}, \bar{v}_{Sx}, 0, \bar{H}, 0\right], \tag{9}$$

such that the nominal impact location is $z = x = 0$.

B. Free Fall

The free fall is governed by a constant gravitational acceleration; we further assume aerodynamic effects to be negligible. Therefore, the ball trajectory is linear in the initial conditions S_0 and the exact mapping of the perturbations over the free fall is

$$s_1 = M_{01} s_0, \tag{10}$$

where

$$M_{01} = \begin{bmatrix} 1 & T & 0 & 0 & 0 \\ 0 & 1 & 0 & 0 & 0 \\ 0 & 0 & 1 & 0 & 0 \\ 0 & 0 & 0 & 1 & T \\ 0 & 0 & 0 & 0 & 1 \end{bmatrix}. \tag{11}$$

The ball state at nominal impact time T (denoted by the subscript 1) is therefore

$$S_1 = \bar{S}_1 + s_1, \tag{12}$$

with

$$\bar{S}_1 = \left[0, \bar{v}_{Sx}, 0, 0, \bar{v}_{Sz}\right]. \tag{13}$$

C. Impact

1) Impact Time Perturbation: The perturbations cause the impact time to be perturbed as well. The impact time is now $T + \tau$. Before we apply the impact equations, we determine τ, which fully defines the ball and paddle impact state. We approximate the motion of the ball to first order in the impact time perturbation τ

$$S(\tau) \approx S_1 + \dot{\bar{S}}_1 \tau = \bar{S}_1 + s_1 + \dot{\bar{S}}_1 \tau, \tag{14}$$

where

$$\dot{\bar{S}}_1 = \left[\bar{v}_{Sx}, 0, 0, \bar{v}_{Sz}, -\gamma\right]. \tag{15}$$

To first order, $\dot{S}_1 \approx \dot{\bar{S}}_1$. Similarly, we approximate the paddle motion

$$P(\tau) \approx \bar{P}_1 + \dot{\bar{P}}_1 \tau. \tag{16}$$

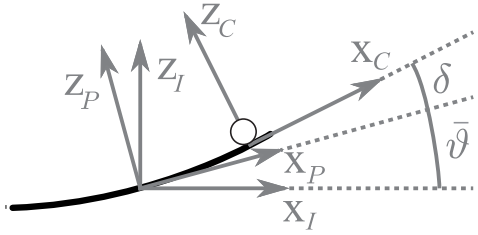

Fig. 3. Parabolic paddle and coordinate systems. At impact, the paddle is at angle $\bar{\vartheta}$ with respect to the inertial coordinate system I. The collision coordinate system C is aligned with the surface normal of the parabolic juggling paddle and is at angle δ with respect to the paddle coordinate system P. The surface of the parabolic paddle satisfies $z_P = \frac{c}{2} {x_P}^2$.

The paddle state is always expressed in the paddle coordinate system P, see Fig. 3. The nominal values are

$$\begin{aligned} \bar{P}_1 &= \left[0, 0, 0, 0, \bar{v}_P\right], \\ \dot{\bar{P}}_1 &= \left[0, 0, 0, \bar{v}_P, a_P\right], \end{aligned} \tag{17}$$

where $a_P = -\gamma/2$ is the paddle acceleration at impact derived in [1]. An impact occurs if the z position of the ball and paddle, expressed in P, coincide. We ignore the ball radius as it is just a constant offset. We also ignore the paddle curvature, as to first order, the paddle is flat. We introduce the row vector $i := [0, 0, 0, 1, 0]$ that selects the z-coordinate of the state vectors. The impact condition is

$$\begin{aligned} 0 &= i A_{PI} S(\tau) - i P(\tau) \\ 0 &= i A_{PI} \left(\bar{S}_1 + s_1 + \dot{\bar{S}}_1 \tau\right) - i \left(\bar{P}_1 + \dot{\bar{P}}_1 \tau\right), \end{aligned} \tag{18}$$

where A_{PI} denotes the rotation matrix that rotates the ball state by $\bar{\vartheta}$ from I to P. To first order, the impact time deviation has no effect on the paddle angle, as the pendulum is nominally at rest. The nominal ball and paddle states cancel out

$$0 = i A_{PI} \bar{S}_1 - i \bar{P}_1, \tag{19}$$

and we obtain the impact time deviation

$$\begin{aligned} \tau &= -\left(i A_{PI} \dot{\bar{S}}_1 - i \dot{\bar{P}}_1\right)^{-1} i A_{PI} s_1 \\ &= \frac{i A_{PI} s_1}{\bar{v}_P + |\bar{v}_S|}. \end{aligned} \tag{20}$$

2) Impact Location: Due to the perturbations, the ball does not hit the paddle in its center. The curvature c of the paddle and impact location x_P determine the angle δ by which the impact coordinate system C is rotated with respect to the paddle coordinate system P, see Fig. 3. The paddle surface satisfies

$$z_P = \frac{c}{2} x_P^2, \tag{21}$$

where the stabilizing paddle curvature is $c = 0.24\,\mathrm{m}^{-1}$ as derived in [1]. It follows that

$$\delta = -\arctan \frac{dz_P}{dx_P} \approx -c\, x_P, \tag{22}$$

to first order. The minus sign stems from the right-hand rule definition of the angle, see Fig. 3. The impact function is

applied in the impact coordinate system C and we define the rotation matrices A_{CP} and A_{CI} that rotate a vector to C from P and I, respectively.

3) Impact Model: For the vertical impact velocities, we use Newton's impact law (7). For the horizontal directions and spin, we use the impact model derived in [13]. The horizontal coefficient of restitution e_x is defined as

$$e_x := -\frac{\dot{\hat{x}}^+ - R\,\omega_y^+}{\dot{\hat{x}}^- - R\,\omega_y^-}, \tag{23}$$

where R is the ball radius and $\dot{\hat{x}}$ is the relative horizontal velocity of the ball to the paddle. The parameter e_x relates the pre-impact $(-)$ velocity of the contact point of the ball to the post-impact $(+)$ velocity. The values of e_x range from -1 to 1. Combined with conservation of angular momentum, we obtain the impact function

$$S^+ = \Gamma\left(S^-, P^-\right) = A_{IC}\left(C_S\,A_{CI}S^- + C_P\,A_{CP}P^-\right), \tag{24}$$

where C_S, C_P are the mappings of the pre-impact ball and paddle state to the post-impact ball state, respectively. The matrices are defined in the collision coordinate system C and are

$$C_S = \begin{bmatrix} 1 & 0 & 0 & 0 & 0 \\ 0 & 1-k & kR & 0 & 0 \\ 0 & \alpha & 1-R\alpha & 0 & 0 \\ 0 & 0 & 0 & 1 & 0 \\ 0 & 0 & 0 & 0 & -e_z \end{bmatrix}$$

$$C_P = \begin{bmatrix} 0 & 0 & 0 & 0 & 0 \\ 0 & k & 0 & 0 & 0 \\ 0 & -\alpha & 0 & 0 & 0 \\ 0 & 0 & 0 & 0 & 0 \\ 0 & 0 & 0 & 0 & e_z+1 \end{bmatrix}$$

$$\alpha = \frac{e_x+1}{1.4R},\; k = \frac{e_x+1}{3.5} \tag{25}$$

We use a solid PA-6.6 (Nylon) ball with a radius of $R = 0.006\,\text{m}$. Made for valve applications, it provides precise roundness and isotropic impact properties that are crucial for sustained juggling. We used the same ball with the Blind Juggler and measured a ball coefficient of restitution of $e_z = 0.8$. The horizontal coefficient of restitution e_x could not be determined from the data [1].

4) Impact Function: The approximate motion of the ball (14) and paddle (16) and impact time deviation (20) define the ball and paddle state before impact:

$$\begin{aligned} S_2^- &= \bar{S}_1 + s_1 + \dot{\bar{S}}_1\tau \\ &= \bar{S}_1 + s_2^- \end{aligned} \tag{26}$$

$$\begin{aligned} P_2 &= \bar{P}_1 + \dot{\bar{P}}_1\tau \\ &= \bar{P}_1 + p_2, \end{aligned} \tag{27}$$

where the subscript 2 denotes the impact time $T+\tau$. We approximate the impact function Γ (24) to first order to obtain the post-impact ball state

$$\begin{aligned} S_2^+ \;\approx\;& \Gamma\left(\bar{S}_2^-, \bar{P}_2\right) \\ &+ \left.\frac{\partial\Gamma\left(S,P\right)}{\partial S}\right|_{\bar{S}_2^-,\bar{P}_2} s_2^- \\ &+ \left.\frac{\partial\Gamma\left(S,P\right)}{\partial P}\right|_{\bar{S}_2^-,\bar{P}_2} p_2 \\ =\;& \bar{S}_2^+ + s_2^+, \end{aligned} \tag{28}$$

where

$$\bar{P}_2 = \bar{P}_1, \quad \bar{S}_2^- = \bar{S}_1, \quad \bar{S}_2^+ = [0, -\bar{v}_{Sx}, 0, 0, -\bar{v}_{Sz}]. \tag{29}$$

D. Free Fall until Apex

After the impact, the ball is in free fall until the nominal apex time $2T$. The free fall is analogous to Section III-B. We reuse M_{01} from (11) to map the perturbations at $T+\tau$ to $2T+\tau$. We obtain

$$S\left(2T+\tau\right) = \bar{S}_3 + M_{01}\,s_2^+, \tag{30}$$

where

$$\bar{S}_3 = [-\Delta\tilde{x}, -\bar{v}_{Sx}, 0, \bar{H}, 0]. \tag{31}$$

The subscript 3 indicates the nominal apex time. In order to obtain the ball state at the nominal apex time $2T$, we compensate for τ analogous to (14)

$$S_3 = \bar{S}_3 + M_{01}\,s_2^+ - \dot{\bar{S}}_3\,\tau, \tag{32}$$

where

$$\dot{\bar{S}}_3 = [-\bar{v}_{Sx}, 0, 0, 0, -g]. \tag{33}$$

Combining the above equations, we obtain the matrix M_{03} that maps the initial perturbations s_0 over a single bounce

$$s_3 = M_{03}\,s_0. \tag{34}$$

This mapping only describes half the trajectory of the ball on the Pendulum Juggler. There is another impact taking place at the opposite peak of the pendulum angle. We may reuse the derived mapping for the second part if we reflect the perturbations

$$\begin{aligned} \hat{s}_3 &= U M_{03}\,s_0 \\ &= \hat{M}_{03}\,s_0, \end{aligned} \tag{35}$$

where U is a diagonal matrix with the diagonal elements $\{-1,-1,-1,1,1\}$. Only the $x, \dot{x}$, and ω_y elements are reflected. The mapping of the perturbations over the full trajectory is $\hat{M}_{03}^2$. A Mathematica file with the derivation of this mapping is available on the project website [14].

E. Stability

The trajectory is locally stable if the spectral radius of $\hat{M}_{03}$ is smaller than 1, which means that the perturbations approach zero as the number of impacts tends to infinity, in the absence of process noise [12]. The spectral radius is defined as

$$\rho\left(\hat{M}_{03}\right) := \max_i |\lambda_i|, \tag{36}$$

where λ_i is the i-th eigenvalue of $\hat{M}_{03}$. Since we could not identify the horizontal impact parameter e_x in previous work [1], we find the worst-case spectral radius over a range of values $e_x \in [-0.5, 0.5]$ and find that

$$\max_{e_x} \rho\left(e_x, \phi\right) \tag{37}$$

is in the interval $[0.90, 0.95]$ over the range of pendulum amplitudes $\Phi \in \left[0, \frac{\pi}{6}\right]$. We used $\Lambda = 1\,\text{m}$ to calculate the horizontal distance $\Delta\tilde{x}$ traveled by the ball.

The stability of the full ball trajectory with two impacts immediately follows as the spectral radius of $\hat{M}_{03}^2$ is ρ^2 and therefore also smaller than 1.

IV. HARDWARE DESIGN

We discuss the design of the four-bar linkage that keeps the paddle perpendicular to the impact velocity of the ball.

A. Design Specifications

Before finding the four-bar linkage parameters, we review the design specifications that we fixed a priori:

1) The pendulum should roughly have a length of 1 m. We found a pendulum period time of $1.882\,\text{s}$ using a physical pendulum of 1 m with a mass corresponding to the linear motor and paddle at its tip. This results in a nominal time from apex to impact of $T = 0.4705\,\text{s}$ and nominal apex height of $\bar{H} = 1.086\,\text{m}$.
2) The desired maximal amplitude Φ of the equivalent pendulum angle ϕ is $\pi/6$ or $30°$, resulting in a horizontal distance traveled by the ball of $\approx 1\,\text{m}$.
3) We control the pendulum's motion with two motors mounted to the top pivot of the four-bar linkage.
4) While it is possible to manually initialize the ball with the Blind Juggler, it would be very hard to get both the timing and horizontal initial ball velocity right with the Pendulum Juggler. We therefore plan to introduce the ball to the system when the pendulum is at rest and start increasing the pendulum amplitude quasistatically until we reach the desired amplitude. This requires the paddle angle to be perpendicular to the impact velocity of the ball over the whole range of pendulum amplitudes from 0 to $\pi/6$.

B. Four-Bar Linkage Design

The relevant angles and design parameters are introduced in Fig. 1. The goal is to find the link lengths a, L, and b of the symmetric four-bar mechanism, such that the paddle is perpendicular to the impact velocity of the ball over the whole range of possible pendulum amplitudes. Furthermore, because the total mass of the motor and paddle at the tip of the pendulum is high (approximately $5\,\text{kg}$), and forcing the pendulum to swing at a frequency different from the pendulum's eigenfrequency would require strong and highly geared motors, the pendulum natural period time should match the flight time of the ball.

We use a Matlab Sim-Mechanics model of the mechanism to find the link lengths a, L, and b. Given a set of parameters, we simulate the mechanism for half a pendulum period

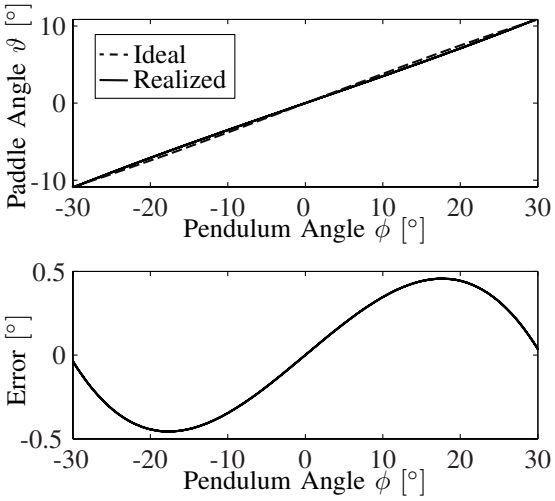

Fig. 4. **Top**: Ideal and realized paddle angle. The link lengths obtained from the optimization result in a close match. **Bottom**: Error in the paddle angle. The maximal error is $\hat{e} = 0.43°$ at a pendulum angle of $\phi = 16°$. We find that a deviation of the mean impact location of just $\frac{\hat{e}}{c} = 0.031\,\text{m}$ would compensate for this error (neglecting the additional horizontal distance to be traveled by the ball).

$2T$ and measure the paddle angle ϑ. We then formulate an optimization problem on the deviation from the ideal angle. Since the upper (a) and lower (b) link lengths have a correlated impact on the paddle angle, we fix the upper link length a to $0.16\,\text{m}$ based on the dimensions of the top pivot structural parts. We then

$$\begin{aligned} \text{minimize} \quad & J\left(b, L\right) \\ \text{s.t:} \quad & L \geq 0 \\ & b \geq 0 \end{aligned}, \tag{38}$$

where the objective function J is defined as

$$J\left(b, L\right) := \int_0^{2T} g\left(t, b, L\right) dt + h\left(2T, b, L\right). \tag{39}$$

The objective function includes the integrated paddle error over half a pendulum period of $2T$ and a final cost penalizing deviations from the nominal impact angle and angular velocity. This results in a trade-off between how close the realized paddle angle matches the ideal angle and how well the natural period of the linkage matches the flight time of the ball. The instantaneous cost

$$g\left(t, b, L\right) := q\left(\phi(t)\right)\left(\vartheta(t) - \bar{\vartheta}\left(\Delta x(t)\right)\right)^2 \tag{40}$$

is the weighted deviation of the measured paddle angle ϑ from the ideal angle $\bar{\vartheta}$, defined in (4). We use the actual distance Δx traveled by the ball, which we measure in the simulation. The distance traveled $\Delta\tilde{x}$, derived from the equivalent pendulum parameters, is not equal to Δx since the linear motor nominal impact extension creates an offset, see Fig. 1. For better readability, we drop the dependence of the angles on the parameters b and L. The weight q is a function of the measured equivalent pendulum angle ϕ. We choose the weight to be

$$q\left(\phi(t)\right) := \left(\phi(t)/\Phi\right)^4, \tag{41}$$

which penalizes paddle angle deviations more if the equivalent pendulum angle ϕ is close to the maximal design amplitude of $\Phi = \pi/6$. We do this to bias the optimization in order to better match the angles where the impact velocities are larger due to higher horizontal velocities. The final cost is

$$h\left(2T, b, L\right) := \left(\phi(2T) - \Phi\right)^2 + \dot{\phi}(2T)^2. \qquad (42)$$

The final cost penalizes deviations from the desired pendulum amplitude Φ and angular velocity at the nominal impact time $2T$, which is equivalent to penalizing deviations of the resulting from the desired pendulum natural period time given the flight time of the ball.

In the model, we ignore the paddle striking motion and assume a fixed extension of the linear motor at the nominal impact position. We use Matlab `fminsearch` and find the minimizing link lengths $b = 0.245\,\text{m}$ and $L = 0.985\,\text{m}$. The realized and ideal paddle angle are compared in Fig. 4.

C. Hardware and Pendulum Control

Given the link lengths, the Pendulum Juggler's geometry is fully defined. We built a prototype using standard aluminum profiles and custom-made pivots with ball bearings. The brushless motors attached to the top pivot axles are Maxon EC-90, which provide up to $0.386\,\text{Nm}$ each. The motors are driven by a Maxon DEC 70/10 amplifier, which we use in torque control mode. The motors are used to control the pendulum's motion, which is subject to disturbances such as the motion of the paddle. As a first and very straightforward approach, we used a tracking proportional controller to act on the error signal

$$e\left(t\right) := \Phi \cos\left(\frac{2\pi}{4T}t + \lambda\right) - \phi\left(t\right), \qquad (43)$$

where Φ is the desired pendulum amplitude and $\phi\left(t\right)$ is the measured equivalent pendulum angle. The phase parameter λ is adjusted after every paddle stroke to make sure that the pendulum and paddle motions remain synchronized. These adjustments are very small. The proportional controller runs at $100\,\text{Hz}$ on a dSpace system [15]. On the same system, we run a finite state machine that provides the timing and parameters of the paddle motion, which is generated by an industrial servo controller.

V. Preliminary Results and Outlook

In experiments with the Pendulum Juggler, we achieved juggling at amplitudes of up to $\Phi = 25°$, as documented in a series of video stills in Fig. 2. In the video accompanying this submission, we also show the process of reaching a desired juggling amplitude by quasistatic transition from $\Phi = 0$. Beyond amplitudes of $25°$, the brushless motors were too weak to keep the pendulum motion synchronized with the striking motion of the paddle, causing the ball to fall off.

We show experimental data measured at the maximal realized juggling amplitude in Fig. 5. The synchronization of the pendulum motion is a very rich control problem. We are currently working on using the paddle motion as an additional control input to the system. The paddle motion is constrained by the striking motions, but in between, it may follow an arbitrary trajectory that could be used to minimize motor control effort or, ideally, make the motors redundant.

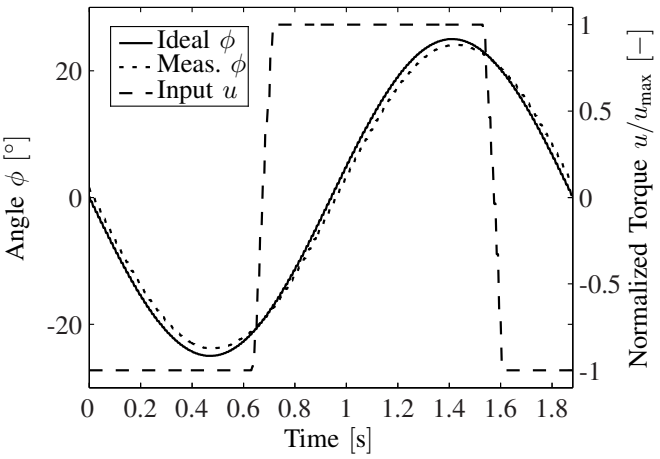

Fig. 5. Measured vs. ideal equivalent pendulum angle ϕ and normalized torque at a juggling amplitude of $\Phi = 25°$. The input saturates at maximum normalized torque.

VI. Acknowledgements

The authors would like to thank Matthew Donovan for his great help with the mechanical design.

References

[1] P. Reist and R. D'Andrea, "Bouncing an unconstrained ball in three dimensions with a blind juggling robot," in *Proc. IEEE Int. Conf. Robotics and Automation (ICRA)*, 2009.

[2] A. Schoellig, F. Augugliaro, S. Lupashin, and R. D'Andrea, "Synchronizing the motion of a quadrocopter to music," in *Proc. IEEE Int. Conf. Robotics and Automation (ICRA)*, 2010.

[3] B. Piccoli and J. Kulkarni, "Pumping a swing by standing and squatting: do children pump time optimally?" *Control Systems Magazine, IEEE*, vol. 25, no. 4, pp. 48 – 56, aug. 2005.

[4] R. R. Burridge, A. A. Rizzi, and D. E. Koditschek, "Sequential Composition of Dynamically Dexterous Robot Behaviors," *Int. J. Rob. Res.*, vol. 18, no. 6, pp. 534–555, 1998.

[5] M. Buehler, D. E. Koditschek, and P. J. Kindlmann, "Planning and control of robotic juggling and catching tasks," *I. J. Robotic Res.*, vol. 13, no. 2, pp. 101–118, 1994.

[6] A. Rizzi and D. Koditschek, "Further progress in robot juggling: the spatial two-juggle," in *Proc. IEEE Int. Conf. Robotics and Automation (ICRA)*, May 1993, pp. 919 –924 vol.3.

[7] P. J. Holmes, "The dynamics of repeated impacts with a sinusoidally vibrating table," *J. Sound Vibr.*, vol. 84, pp. 173–189, Sep. 1982.

[8] S. Schaal and C. Atkeson, "Open loop stable control strategies for robot juggling," in *Proc. IEEE Int. Conf. Robotics and Automation (ICRA)*, 1993.

[9] R. Ronsse, P. Lefevre, and R. Sepulchre, "Sensorless stabilization of bounce juggling," *IEEE Transactions on Robotics*, vol. 22, no. 1, pp. 147–159, Feb 2006.

[10] ——, "Rhythmic feedback control of a blind planar juggler," *IEEE Transactions on Robotics*, vol. 23, no. 4, pp. 790–802, Aug 2007.

[11] H. Miyamoto, A. Sano, Y. Ikemata, S. Maruyama, and H. Fujimoto, "A study of bouncing rod dynamics aiming at passive running," in *Proc. IEEE Int. Conf. Robotics and Automation (ICRA)*, 2010.

[12] S. H. Strogatz, *Nonlinear Dynamics And Chaos*, 1st ed. Perseus Books Group, January 1994.

[13] R. Cross, "Grip-slip behavior of a bouncing ball," *Amer. J. Physics*, vol. 70, no. 11, pp. 1093–1102, 2002.

[14] [Online]. Available: http://www.blindjuggler.org

[15] [Online]. Available: http://www.dspace.de